

Modification of Plastic Scintillator for Neutron Registration

P. Zhmurin^(✉)

Institute for Scintillation Materials, NAS of Ukraine,
60 Nauki Ave., Kharkiv 61001, Ukraine
{zhmurin, boyanrintsev}@isma.kharkov.ua

Abstract. The paper presents the main results of neutron sensors development on the base on the plastic scintillators (PS). The role of the excitation energy in the neutrons detection. It has been established that the ability of the neutron gamma separation significantly improves with an increase in the concentration of the activator molecules, but at the same time leads to a considerable degradation of its mechanical properties. It is shown that the use of sterically modified molecules as an activator of the polymer base not only does not impair the properties of gamma separation neutron but also leads to a significant improvement of mechanical properties of PS.

1 Introduction

The plastic scintillators are widely used for registration of high-energy charged particles and gamma rays. The polymers, having in composition a fragment with π -conjugated electrons, can be used as base plastics scintillators [1]. Other words polymer base should have chromophore groups that possess with luminescence at a varying degree. In addition, the polymers should maintain high optical quality for the large chunk polymerization; have long-term stability and accessibility for tooling. Despite the huge list of known polymer media, only polystyrene and polyvinyl toluene are used for industrial production. In such molecules benzene groups act as chromophores, which have three allowed transitions, 180, 200 and 250 nm.

The polymers contain sufficiently large amount of hydrogen atoms and thus neutrons effectively interact with them by scattering on protons (hydrogen nuclei). Wherein, protons produce scintillation pulse, which does not differ from the scintillation pulse from gamma rays. Therefore, plastic scintillators in their conventional form are not suitable for neutron-gamma separation. Therefore, it is necessary to modify the composition of the PS for such goal. Note, the pulse shape discrimination (PSD) is the most effective method for neutron detection in organic media.

For high-energy particle interaction with the organic medium the track can be represented as a set of separate areas, in which a secondary electron thermalization takes place. The size of this areas is considerably lower than Onzager radius, so the secondary electron has to recombine with a geminate ion. Therefore, particles with low energy losses density (the case of the electron thermalization areas overlapping), excitation energy is concentrated mainly in the singlet state. With increasing the energy

density losses, the electron thermalization areas start overlapping. Hence there is a possibility of the recombination of electrons with not geminated ions. As a result, there is a possibility of the formation of the triplet excited states, which lifetime is much longer than the lifetime of the singlet excited states. Therefore, the fast and slow components separation allows to discriminated energy distribution between the singlet and triplet subsystems. So, the fast and slow components ratio can be used as the criterion for particle discrimination (n/γ -discrimination in particular) [Error! Bookmark not defined.]. Such PSD analysis is efficient to register a fast neutron on gamma-ray background with organic scintillators (stilbene crystals, liquid scintillators) [2].

The best and most typical organic scintillators for neutrons and gamma-quanta discrimination by PSD are stilbene, anthracene, p-terphenyl, and others [2–4]. The typical figure of merit (FOM) for stilbene amounts is 4.7 [5], although for the statistically reliable neutrons and gamma-quanta pulse shape discrimination FOM will be not less than 1.27, that corresponds to uncertainty 3σ [5].

Also, the liquid scintillators, as NE-213, NE-230, NE-232, and their analogs have some less meaning for the pulse shape particle discrimination (FOM = 3.1) [5–7].

Despite high n/γ -discrimination, the organic scintillators have some significant disadvantages, that limit their applications. The limits for single crystals are small sizes, difficulties of the growth, tooling and their high cost. Disadvantages of liquid scintillators are the low ignition temperature, inconvenience in use relatively to the solid-state detectors.

Plastic scintillators (PS) are free from such disadvantages, but commercial PS for pulse shape n/γ -discrimination are not presented in the market and are not produced by industry nevertheless were made repeatedly. This is because the lifetime of triplet excited states of polystyrene chromophore groups is comparable with the lifetime of the singlet states and the scintillation pulse in PS does not have any slow component and PSD is not realized.

So for the PSD plastics it is necessary to display the triplet excitation energy. There are two ways for realization. The first is related to the possibility of creating chromophore groups with long-living triplet states in the PS polymeric medium, on which the triplet-triplet annihilation can be realized. The other one relates to presence of activators in the PS polymeric medium, able to collect effectively the triplet excitation energy. While the PSD using the first way is made by this time, the possibility to create the new PS using the other way was not tried.

2 Direct Harvesting of Triplet Excited States Energy

It is necessary to create two activation centers to realize the PSD in PS by direct collection of the excited triplet states in the polymer. The first is based on traditional organic dyes, that collect the singlet states excitation. An other one is based on organic metal complexes that are characterized by the strong spin-orbit interaction, and they have the possibility of collecting the excitation energy from the triplet states.

The dibenzoilmethanate-Eu-1,10-phenanthroline europium complex (Eu [DBM]₃Phen) has been selected as effective activator for collection of excitation energy from the triplet states of the PS [8, 9] (Fig. 1).



Fig. 1. The PS activated by the dibenzoilmethanate-Eu-1,10-phenanthroline europium complex under UV-irradiation

At first sight, it was obvious to use for fast component formation the same activators, which are traditionally used in the composition of conventional PS. But it was found, that the PS activated with 2 wt% *p*-terphenyl (*p*-TP) and 2 wt% Eu [DBM]₃Phen do not have the fast pulse component, produced by *p*-TP. Moreover *p*-TP luminescence is also not observed by the photo excitation of the PS with 265 nm wavelength, that corresponds to the maximum absorption of polystyrene. It means that the presence of the Eu[DBM]₃Phen complex in amount of 2 wt% in polystyrene solid solution suppresses completely the *p*-TP luminescence. The situation is similar to other known activators like PPO, PBD etc. The analysis (Fig. 2) reveals unsuitability of the traditional phosphors for using as activators together with the Eu[DBM]₃Phen complex due to the small Stokes shift of the usual activators.

So, it is necessary to search the fluorescent activator with the absorption spectra coinciding with the polystyrene and with long-wavelength luminescence, that is mismatched with the Eu[DBM]₃Phen complex absorption. It was shown [10, 11] that 1,4-dimethyl-9,10-diphenylanthracene (DMDPA) corresponds to the specified requirements. The formula of the diphenylanthracene is presented at Fig. 3.

From the comparison of Figs. 2 and 4 it is seen, that the DMDPA luminescence is located outside of the absorption band of Eu[DBM]₃Phen and does not suffer the absorption. Thus, DMDPA is suitable for use as the activator for singlet excitation collection in the presence of Eu[DBM]₃Phen. The presented composition can be used to create PS with the n/γ pulse shape discrimination.

2.1 Preparation of PS with Eu Complex for n/γ -Discrimination

PS were prepared by thermal polymerization in a sealed vial [10, 11]. Necessary amount of additives (0.3 g) was placed into an ampoule of thermal proof glass 18 mm

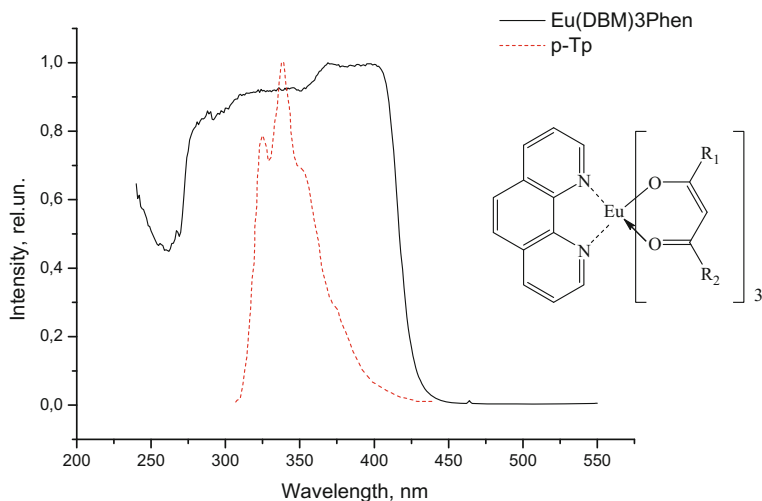


Fig. 2. The excitation specter of polystyrene film with 2 wt% Eu[DBM]₃Phen content (solid line), and the luminescent specter of polystyrene film with 2 wt% p-Tp content (dashed line). The observation wavelength 612 nm, excitation—262 nm. On the right—the structural formula Eu [DBM]₃Phen

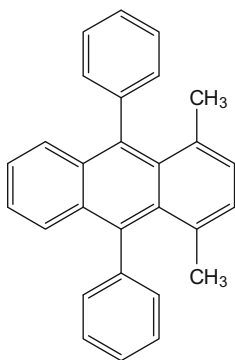


Fig. 3. The formula of substance 1,4-dimethyl-9,10-diphenylanthracene (DMDPA)

in diameter and fresh distilled styrene was added to the solution mass of 10 g. The vial was heated to the temperature $T = 35\text{ }^{\circ}\text{C}$ to dissolve it. Then it was purged with argon for 6 min. After this stage the vial was sealed and placed into a thermostat at the temperature of $80\text{ }^{\circ}\text{C}$ and held for 96 h. After holding, the thermostat was cooled to $40\text{ }^{\circ}\text{C}$ at the rate of $5\text{ }^{\circ}\text{C/h}$. After cooling to room temperature, the sample was taken out from the vial. Obtained PS samples with cylindrical shape of 16 mm in diameter and of 10 mm in height were polished all sides to optical purity.

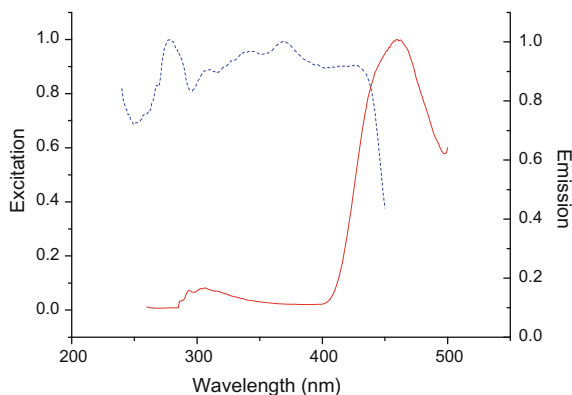


Fig. 4. The excitation (dashed line) and luminescence (solid line) specters of polystyrene film, containing 1.5 wt% DMMPA. The observation wavelength 461 nm, excitation—265 nm

Content of the PS was varied in limits, wt%:

Eu[DBM] ₃ Phen	2.5–3.5
DMDPA	0.7–1.5
Polystyrene	Rest

2.2 The n/γ -Discrimination Parameter FOM

Measurement of FOM for PS with n/γ -discrimination able to collect singlet and triplet states, was carried out by the PMT Hamamatsu R669 with the extended to the red area sensitivity, because the Eu[DBM]₃Phen additive luminescence is at the red range (612 nm). This additive luminescence forms the slow (triplet) component of the scintillation pulse with the decay time $\tau = 370 \mu\text{s}$. The fast (singlet) component with decay time $\tau = 13 \text{ ns}$ is formed by the DMDPA additive luminescence. So, the fast decay time is in 30,000 times shorter than the slow component. For simultaneous registration of both components with an oscilloscope, the PMT anode signal discharge time was lengthened to $\tau = 15 \mu\text{s}$. It was reached by the anode load value with $R_a = 51 \text{ k}\Omega$. The signal from the anode load was connected to the both channels of a digital oscilloscope Rigol DS1302CA (300 MHz, 2Gsample, 8 bit of the vertical scale). The inner input load of the both channels was set to $1 \text{ M}\Omega$. The first channel sensitivity was 20 mV/div, the other was 5 mV/div, the horizontal sweep was $50 \mu\text{s}/\text{div}$, the synchronization delay time was 250 μs .

Figure 5 presents the new PS average normalized digital oscillograms, obtained by registration of α -particles from a Pu-239 source with the energy $E_\alpha = 5.4 \text{ meV}$ and electrons from a Bi-207 source with the energy $E_e = 0.975 \text{ meV}$. The oscillograms are obtained at the PMT anode load $R_a = 51 \text{ k}\Omega$. It is seen (Fig. 5), that the oscillogram amplitude varies in 1000 times. It is shown that the α -particles and electrons pulse shapes are significantly different that qualitatively demonstrates an ability to n/γ -discrimination.

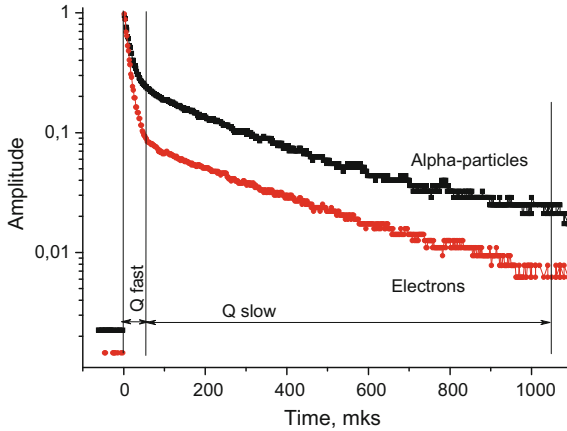


Fig. 5. Average normalized pulse of new PS under α -particles from Pu-239, $E_\alpha = 5.3$ MeV (the higher curve) and under electrons from Bi-207 $E_e = 0.975$ MeV (the lower curve) irradiation. The PMT anode load resistance $R_a = 51$ k Ω

Data were transmitted from the digital oscilloscope to a computer, where they were stored and processed by a special software. In an output file, the fast and slow pulse components square values Q_{fast} and Q_{slow} were saved. Then ratio— $R = Q_{slow}/Q_{fast}$ was calculated for each event and then the dependence Q_{slow}/Q_{fast} on Q_{fast} was estimated. Also the distribution of the value $R = Q_{slow}/Q_{fast}$ was obtained.

Figure 6 demonstrates the dependence Q_{slow} from the Q_{fast} for the polystyrene based PS with 3.0 wt% Eu[DBM]₃Phen and 1.0 wt% DMDPA is presented. PS sample had an optical contact with the PMT input window and was irradiated by fast neutrons (Pu–Be source through a 10 mm thick lead plates). Two groups of points are seen. The higher group is associated with the registered neutrons (recoil protons); the lower one—to γ -rays (Compton electrons). Two groups do not intersect. That means good quality of n/γ -discrimination of the new type PS.

For quantitative estimation of n/γ -discrimination, FOM was calculated. The dependence Q_{slow}/Q_{fast} on Q_{fast} is presented at Fig. 7. The higher abscissa in Fig. 7 is scaled in electrons energy values, respective to Q_{fast} . Q_{fast} electron energy calibration was performed with conversional electrons with the energy $E_e = 975$ keV from a Bi-207 source.

Figure 7 demonstrates the neutrons and γ -ray are clearly separated. The Q_{slow}/Q_{fast} values are located in two groups with weight centers at $R \sim 1.0$ and ~ 0.8 , which respect to neutrons and γ -rays. At the value $R = Q_{slow}/Q_{fast} > 0.81$ neutrons are observed and at $Q_{slow}/Q_{fast} < 0.81$ — γ -rays. Thus, if the pulses distribution Q_{slow}/Q_{fast} is estimated, then information about relative location and intersection of Q_{slow}/Q_{fast} is obtained as the result of statistical analysis.

The pulses distribution on the Q_{slow}/Q_{fast} value is presented at Fig. 8. The left peak is associated with gamma-rays, and the right one—to neutrons. FOM is calculated accordingly to the formula: $FOM = \frac{xc2 - xc1}{FWHM1 + FWHM2}$, where xc1 and xc2 are locations of

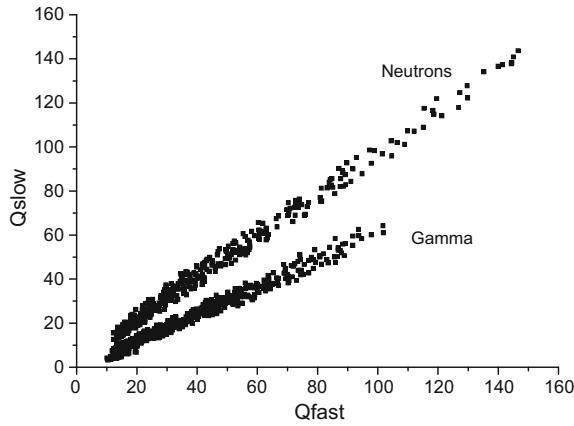


Fig. 6. Dependence Q_{slow} on Q_{fast} measured with the polystyrene PS with 3.0 wt% Eu [DBM]₃Phen and 1.0% DMDPA content. Excitation was performed with fast neutrons and γ -rays from a Pu–Be source through a lead plate 10 mm thick

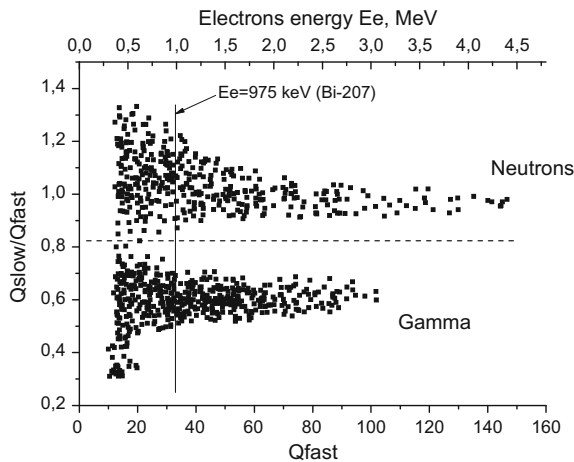


Fig. 7. Dependence of relation $R = Q_{\text{slow}}/Q_{\text{fast}}$ on Q_{fast} for the PS sample with 3.0 wt% Eu [DBM]₃Phen, 1.0 wt% DMDPA content. Excitation was performed with fast neutrons and γ -rays from a Pu–Be source through a lead plate 10 mm thick. The registration trigger level is according to the electron-equivalent energy $E_{\text{ee}} = 350$ keV

the centers. FWHM1 and FWHM2 are the full width on half of the height of the gamma and neutron peaks respectively. The calculations were carried out for all events with the energy more than 350 keV by electron scale.

Thus, the PS for PSD with direct radiation of triplet excitation energy, with 3.0 wt% Eu[DBM]₃Phen and 1.0 wt% DMDPA content, provide statistically reliable pulse shape n/γ -discrimination with $FOM = 1.37$ for particles with the energy $E_e > 350$ keV by electron scale.

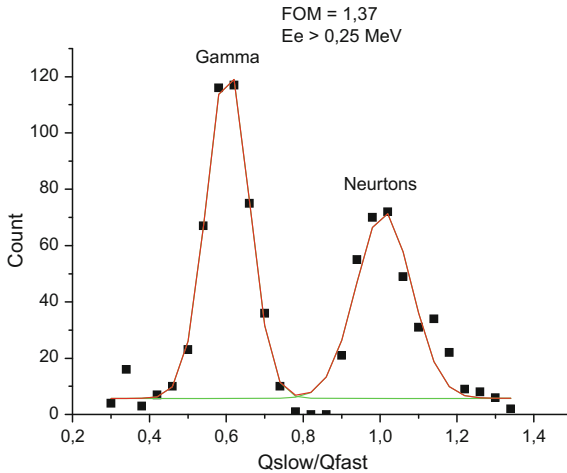


Fig. 8. $Q_{\text{slow}}/Q_{\text{fast}}$ value distribution of events with $E > 350$ keV (in electron-equivalent scale). PS content—3.0% Eu[DBM]₃Phen, 1.0% DMDPA. Dots—experiment, solid line—Gaussian approximation. FOM = 1.37

The PS for PSD with direct radiation of triplet excitation energy, with 3.0 wt% Eu [DBM]₃Phen and 1.0 wt% DMDPA content, provide statistically reliable pulse shape n/γ -discrimination with FOM = 1.37 for particles with the energy $E_e > 350$ keV by electron scale.

3 Triplet-Triplet Annihilation Use for Conversion of Triplet Excited States Energy to Light

In [5] PS based on polyvinyltoluene for n/γ -discrimination with the high primary additive—up to 37 wt% of 2,5-diphenyloxazole (PPO) was developed. This PS had the FOM = 3.31, that was close to commercial LS EJ-301 (FOM = 3.21) [5]. The high n/γ -discrimination rate was reached due to high PPO content. That allowed to increase significantly the triplet-triplet annihilation process probability. As a result, the pulse long component and the n/γ -discrimination parameter were upscaled. It is necessary to notice, the high PPO content in this PS, close to the solubility threshold, leads to decrease of the PS transparency, mechanical hardness, and long-term stability [12]. That limits its use and makes its cost close to the organic single crystals cost.

From the presented short review it can be concluded, that all known PS for n/γ -discrimination have significant disadvantages, which inhibit their production. These disadvantages are connected with the impossibility of polymerization of compositions, containing high activator amount.

3.1 Development of a PS for n/γ -Discrimination with Increased Mechanical Strength

In [5] the PS with the high PSD scintillator is presented. However, investigation of this PS properties showed, that material is very soft and difficult in tooling. In addition, intensive diffusion of PPO activator from the PS volume and its condensation on the surface are observed. It means that this PS is not convenient in practice. Thus, it is necessary to develop PSD PS with increased mechanical strength.

In order to reach the goal it was necessary to find an activator which has high solubility in polystyrene and minimally influences to the mechanical hardness of polymeric matrix. Finally it was found that only PPO between a lot of known activators [Error! Bookmark not defined.] has the proper solubility in vinylaromatic polymers. It is predictable, because the main parameter of a general purpose PS is the scintillation efficiency, the maximum of which is reached at low activator content (1.5–2.0 wt%). In fact, an activator, p-terphenyl and diaryl substituted of oxazole and oxadiazole are used [Error! Bookmark not defined.]. The introduction of polar groups into these systems or π -electron system widening with desired change of the spectral characteristics often leads to decreasing of solubility up to few wt%. Thus, search of a high solubility activator is limited by alkyl- and diaryl-derivatives of oxazole and oxadiazole, because the introduction of alkyls into aromatic phosphor can increase significantly their solubility in such nonpolar organic medium as polystyrene. The diaryl substituted oxadiazole with alkyl groups is the most appropriate substance to improve PS properties.

In Table 1 a set of activators, that are alkyl derivatives of 2,5-diphenyl-1,3,4-oxadiazole (PPD), their melt temperatures, solubility in polystyrene at the room temperature is presented. Activators solubility was performed by the method of thermal polymerization of activator solution in styrene at the different activator concentration (the polymerization regimes are presented below).

The substance solubility in polystyrene is increased with decrease of the melt temperature as it shown at Fig. 1. Wherein, relatively low melt temperature (95 and 85 °C) and, simultaneously, high solubility in polystyrene (40 wt%) are inherent in only two substances—tert-BuPPD and m-DMePPD (Table 1, substances 4 and 7). They were used as activators in preparation of PS with n/γ -discrimination. All samples were prepared on polystyrene base and spectra shifting additive (shifter) 1,4-di-(2-(5-phenyloxazolyl))-benzole (POPOP) in amount of 0.1 wt% was used

PS samples were prepared by thermal polymerization method. Polystyrene-based PS samples were prepared with three different compositions with maximally possible activator content, that limited by the solubility threshold: 40% tert-BuPPD + 0.1% POPOP; 40% m-DMePPD + 0.1% POPOP and 36% PPO + 0.1% POPOP (below the noticed compositions will be signed with abbreviates: 40% TBPPD, 40% DMePPD and 36% PPO). While further activator content increase PS material softening and opacity, areas of unsolved substance on the PS surface are observed. Activator content decreasing leads to n/γ -discrimination properties reduction [5] (Fig. 9).

The micro hardness (HV) of PS was measured by the Wickers method. Long-term stability of PS was determined visually, by the time of additive layer origination on the only just polished PS surface.

Table 1. The melting temperature (T_m) and the solubility of alkyl-derivatives of 2,5-biphenyl-1,3,4-oxadiazole (PPD) in polystyrene at the temperature $T = 293\text{ }^\circ\text{C}$

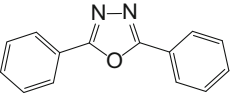
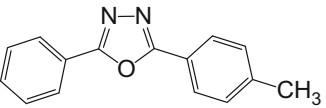
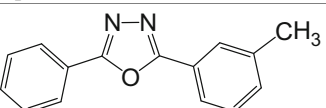
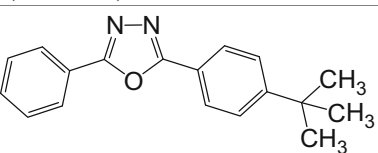
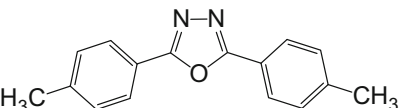
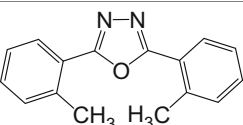
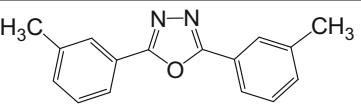
The number of an activator	Name and formula of an activator	The melting temperature T_m ($^\circ\text{C}$)	The solubility at $T = 293\text{ }^\circ\text{C}$ (wt%)
1	 2,5-diphenyl-1,3,4-oxadiazole (PPD)	138	10
2	 2-phenyl-5-(p-tolyl)-1,3,4-oxadiazole (p-MePPD)	125	15
3	 2-phenyl-5-(m-tolyl)-1,3,4-oxadiazole (m-MePPD)	115	15
4	 2-phenyl-5-(4-tert-butylphenyl)-1,3,4-oxadiazole (tert-BuPPD)	95	40
5	 2,5-di-(4-methylphenyl)-1,3,4-oxadiazole (p-DMePPD)	175	4
6	 2,5-di-(2-methylphenyl)-1,3,4-oxadiazole (o-DMePPD)	125	8
7	 2,5-di-(3-methylphenyl)-1,3,4-oxadiazole (m-DMePPD)	85	40



Fig. 9. PSD PS (25 mm diameter and 70 mm height) with 40% TBPPD

The PS scintillation efficiency was determined relatively to a polystyrene based PS with 2 wt% p-TP and 0.02 wt% POPOP by irradiation with monoenergetic electrons with the energy of 975 keV from Bi-207 radionuclide.

The n/γ -discrimination parameter FOM was determined by the method of comparison of charges of whole pulse (Q_{total}) and its delayed component (Q_{slow}) [13, 14]. The scintillation setup consisted of Hamamatsu R1307 PMT and a digital oscilloscope Rigol DS1302CA (300 MHz, 2 GS/s, 8 bit vertical sweep).

PS samples were covered with polytetrafluorethylene light-reflecting film 0.2 mm thick [15] and set with optical contact on the input PMT window. The sample was irradiated with fast neutrons and γ -rays from a Pu–Be source through a lead plate 20 mm thick. The pulse current channel was connected with the both channels of a digital oscilloscope in order to increase the input signal vertical discretization. The input load resistances of the first and second channels were 50 Ω and 1 M Ω , and sensitivities were 50 mV/div and 1 mV/div respectively. The resulting input signal discretization was 13 bit. The horizontal sweep was set equal 50 ns/div, the sweep trigger—from the first channel, normal, the trigger level—6 mV. Digital data from the oscilloscope buffer were transferred by the USB-port to the computer for storage and handling. With the help of a special software the input PMT pulse shape was recovered by coupling of the first and second channel signals. Then the squares of the whole pulse S_{total} and its delayed component S_{slow} were calculated in units [V ns]. Q_{total} and Q_{slow} can be expressed in [V ns] too, because of proportionality of the total current pulse charge to the square under the pulse:

$$Q = \frac{1}{R_{load}} \int_0^{\infty} I(t) dt,$$

where Q is the charge, R_{load} —the load resistance, $I(t)$ – the pulse current function, t —time.

Q_{slow} was measured in the time interval 70 ns from the pulse maximum to 400 ns from the pulse start, Q_{total} —in interval 0–400 ns from the pulse start. In the final file were saved number pairs of Q_{total} and Q_{slow} for every registered pulse.

The n/γ -discrimination parameter FOM is determined for a chosen interval ΔQ_{total} from pulse distribution of Q_{slow} , or from distribution of $R = Q_{\text{slow}}/Q_{\text{total}}$, accordingly to formula: $\text{FOM} = S/(\delta_{\text{gamma}} + \delta_{\text{neutron}})$, where S —the distance between neutron and gamma peak centers of distribution of Q_{slow} or of R , δ_{gamma} and δ_{neutron} —the width on half-height of according peaks [16].

The interval ΔQ_{total} is chosen accordingly to the registered particles energy range, for which FOM is calculated. Due to that two kind particles are registered (neutrons by recoil protons, and γ -rays by Compton electrons), the signal value Q_{total} from every particle is usually expressed in units of the electron-equivalent energy E_{ec} (keVee, MeVee). Spectrometer energetic scale calibration is usually performed with γ -radiation of different sources by Compton edge of monoenergetic γ -rays.

A more precise method of calibration is connected with using of monoenergetic electrons. It is applicable, if the electron energy is totally absorbed in PS material. This means that the PS sample width will be have enough thick for the total electron stop in PS material and its input window must be enough thin to be transparent for electrons. For example, if for spectrometer calibration electrons with the energy of 1 meV, which have the run length is 4.48 mm [17], then the PS sample must be not less than 5 mm thick. The PS samples that was studied in this work correspond to these requirements. The PS input window (polytetrafluorethylene light-reflecting film 0.2 mm thick) is thin, and the PS thickness (15 mm) is enough to absorb electrons with the 3 meV energy. So the electron-equivalent energetic scale calibration was performed with monoenergetic inner conversion electrons from sources Bi-207 (482 and 975 keV) and Cs-137 (624 keV) for every studied of PS sample.

The electron-equivalent energy scale calibration procedure for the PS 36% PPO is illustrated in Fig. 10, where the registered electrons spectra from sources Cs-137 (Fig. 10a) and Bi-207 (Fig. 10b) are presented. The peak maximum locations associated with electrons energy E_e [(624 keV—42.9 V ns (Cs-137); 482 keV—33.3 V ns and 975 keV—68.4 V ns (Bi-207)] were determined by fitting the Gauss function. The result of linear approximation of these data established proportionality between the electron energy E_e and the pulse square Q_{total} : $E_e = -8.61 + 14.45 Q_{\text{total}}$, (Fig. 10c).

3.2 The PS for n/γ -Discrimination Properties

Figure 11 demonstrate dependences of Q_{slow} on Q_{total} for the three PS samples with 40% TBPPD (a), 40% DMPPD (b) and 36% PPO (c) These data were obtained by registration of neutrons and γ -rays from a Pu–Be source. In all cases two groups of results are clear visible.

For quantitative estimation of n/γ -discrimination parameters for PS the FOM parameter was studied for different energies by the method [16]. Events were chosen according to narrow electron-equivalent energy range ΔE_{ec} . Then chosen events distribution on Q_{slow} was estimated.

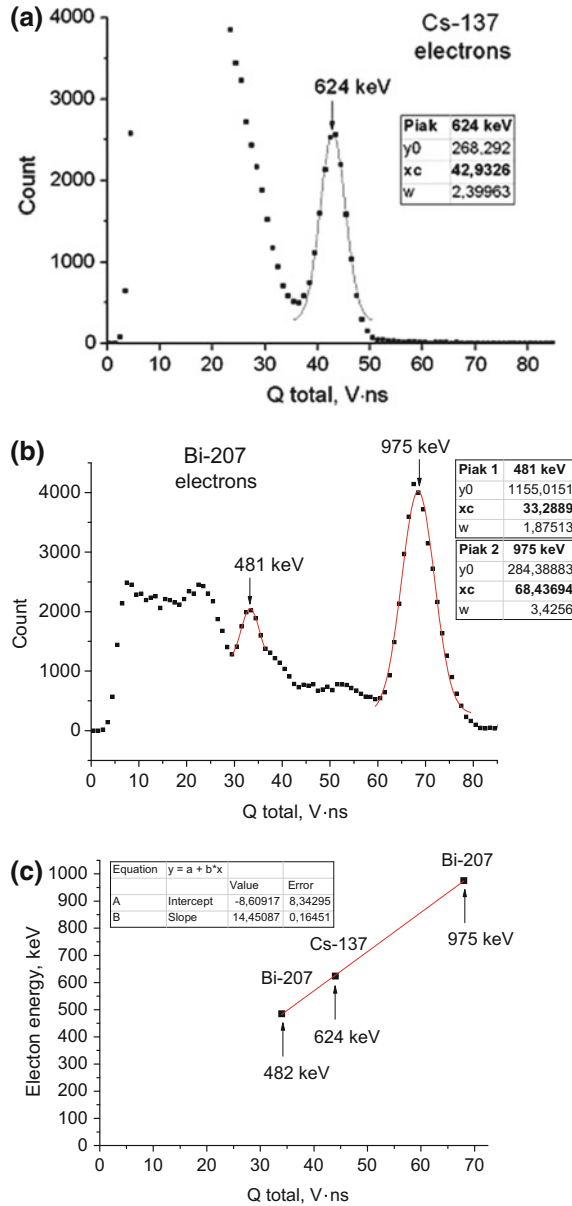


Fig. 10. Electron-equivalent energy scale for the PS 36% PPO. The electron specters from sources Cs-137 (a) and Bi-207 (b). Linear approximation of electron energy dependence E_e on Q_{total} (c)

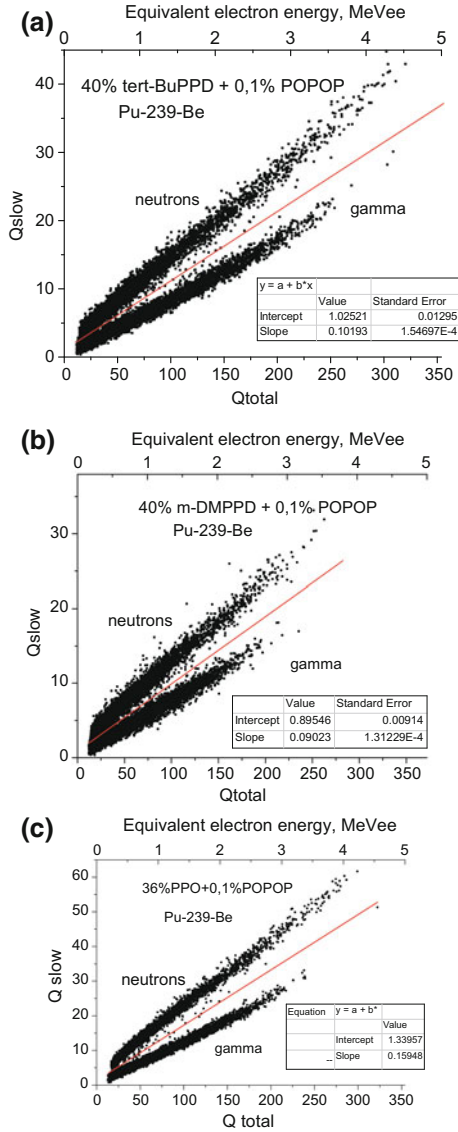


Fig. 11. Dependences of Q_{slow} on Q_{total} for the PS: **a** 40% TBPPD; **b** 40% DMcPPD; **c** 36% PPO. The data obtained by registration of fast neutrons and γ -rays from a ^{239}Pu -Be source. The linear fitting is shown by solid line

In order to eliminate tests disadvantage we used (as at [5]) distribution of Q_{slow}/Q_{total} on Q_{total} , which is practically constant at the energies $E_{ee} \geq 1$ meV but significantly varies at lower energies. That is shown at Fig. 12 where distribution of Q_{slow}/Q_{total} on Q_{total} for the PS 36% PPO is presented (Fig. 13).

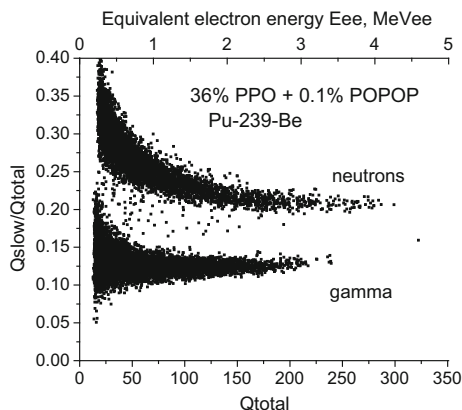


Fig. 12. Dependence of $Q_{\text{slow}}/Q_{\text{total}}$ on Q_{total} for the PS 36% PPO. Data for the fast neutrons and γ -rays. Pu-239–Be source

Thus [18, 19], for FOM calculation, “normalized” dependence of $Q_{\text{slow}}/\langle Q_{\text{slow}} \rangle$ on Q_{total} where $\langle Q_{\text{slow}} \rangle = a + b \cdot E_{\text{ee}}$ —fitting function of dependence of Q_{slow} on Q_{total} was used. The $\langle Q_{\text{slow}} \rangle$ function is shown in Fig. 11c as a solid line which separates neutrons and γ -rays dots groups.

Dependences of $Q_{\text{slow}}/\langle Q_{\text{slow}} \rangle$ on Q_{total} for the PS 40% TBPPD, 40% DMPPD and 36% PPO (see Fig. 12) demonstrate slight shift of $Q_{\text{slow}}/\langle Q_{\text{slow}} \rangle$ in whole energy range for neutrons and γ -rays. That allows to decrease influence of the ΔE_{ee} range to the FOM value.

To determine the FOM Q_{total} and Q_{slow} pairs was sorted on Q_{total} . Then events were chosen in the range $\Delta E_{\text{ee}} = \pm 0.05\%$ of E_{ee} , and selected events distribution of $Q_{\text{slow}}/\langle Q_{\text{slow}} \rangle$ values was obtained. For example, Fig. 14 demonstrates the events distributions on $Q_{\text{slow}}/\langle Q_{\text{slow}} \rangle$ for PS 40% TBPPD and built in three energy ranges— $\Delta E_{\text{ee}} \pm 5\%$ (0.29–0.31; 0.76–0.84 and 1.9–2.1) MeV.

The left peaks correspond to γ -rays. The right peaks correspond to neutrons. The FOM values are be equal to 1.05, 1.56, and 2.0, as it shown at Fig. 14. The FOM values, calculated for different electron equivalent energies E_{ee} , are presented at Table 2 and Fig. 15.

The n/γ -discrimination parameter rapidly grows with registered particles energy increase up to about 1 MeVee (Fig. 15). This growth becomes slower. As it was noticed above, for statistically reliable discrimination, FOM must be more than 1.27. For PS 40% TBPPD, 40% DMePPD and 36% PPO this condition is true at $E_{\text{ee}} \geq 0.5$, 1.25 and 0.2 MeVee respectively.

Results of relative scintillation efficiency, energy resolution, n/γ -discrimination parameter, microhardness and long-term stability for PS are presented at Table 3. Scintillation efficiency of all PS is rise up to more than 11% relatively to the standard PS with 36% PPO (Table 3, sample 4). The energy resolution is improved (about 6%) as well.

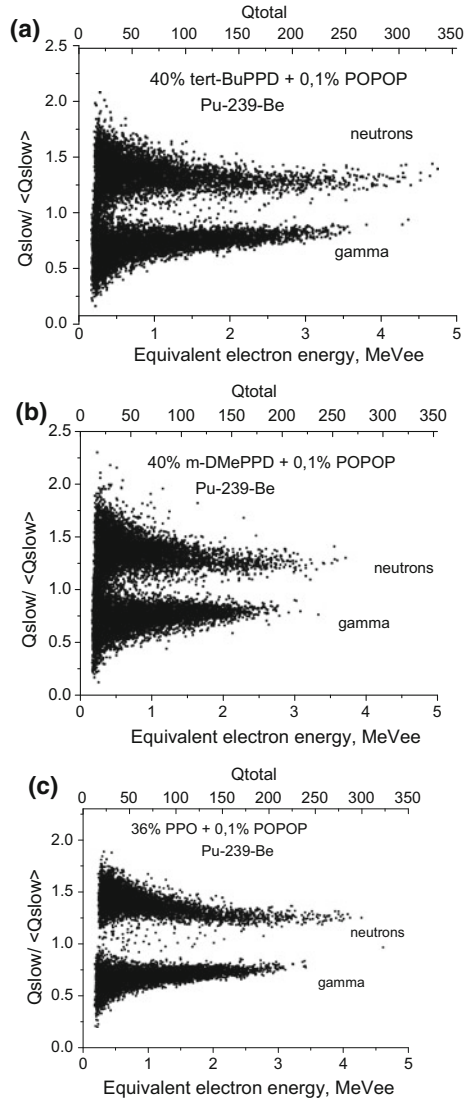


Fig. 13. Dependence of $Q_{\text{slow}}/\langle Q_{\text{slow}} \rangle$ on Q_{total} for the PS: **a** 40% TBPPD; **b** 40% DMePPD and **c** 36% PPO. Data for Pu-239–Be source

Microhardness and the n/γ -discrimination parameter FOM significantly are changes depending on molecule structure and activator concentration. The lowest stability corresponds to the PS with 36% PPO. The highest microhardness is inherent to “standard” PS with the lowest activator (2 wt% p-TP) content: $HV = 231$ MPa. The lowest microhardness $HV = 21$ MPa is inherent to the PS with 36% PPO, the molecule of which has no substitutes and has the simplest structure. The activator molecules with alkyl substitutes TBPPD and DMePPD have more branchy structure relatively to the

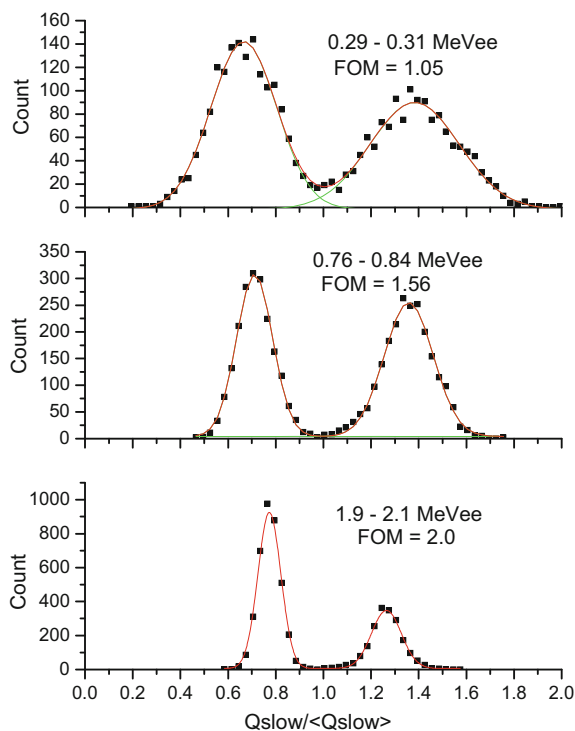


Fig. 14. Distribution of events on $Q_{\text{slow}}/\langle Q_{\text{slow}} \rangle$ for the PS with 40% tert-BuPPD + 0.1% POPOP for different electron-equivalent range— $\Delta E_{\text{ee}} = \pm 0.05\%$ of E_{ee} . Left and right peaks corresponds to γ -rays and neutrons (^{239}Pu -Be source) respectively. Dots—experimental values, solid lines—approximation with couple of Gauss functions

Table 2. The FOM for the three PS, measured at different electron-equivalent energies E_{ee}

E_{ee} (MeVee)	Figure of merit (FOM)			
	40% TBPPD	40% DMePPD	36% PPO	2% p-TP
0.3	1.05	0.68	1.54	
0.4	1.19	0.82	1.75	
0.6	1.43	0.99	2.02	
0.8	1.56	1.13	2.24	0.72
1	1.67	1.22	2.41	0.49
1.5	1.85	1.38	2.75	0.72
2	1.99	1.50	2.96	0.89
2.5	2.15	1.63	3.23	0.97

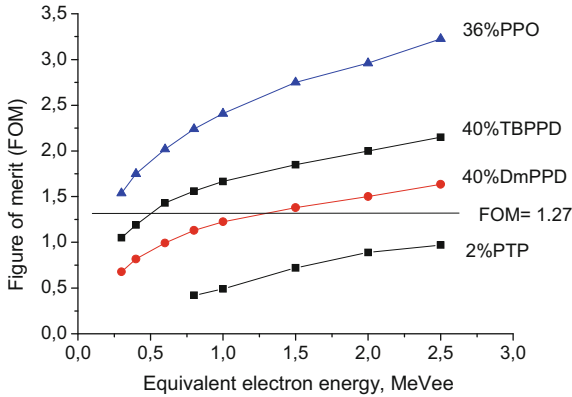


Fig. 15. Dependence of n/γ -distribution FOM on the energy E_{ee} for the PS 40% TBPPD, 40% DMePPD, 36% PPO and 2% p-TP. (Pu-239–Be source). The horizontal line corresponds to FOM value—1.27 at which deviation of n/γ -discrimination is $3(\sigma_{\text{gamma}} + \sigma_{\text{neutron}})$ where σ_{gamma} and σ_{neutron} —standard deviations of γ -rays and neutrons peaks

Table 3. The relative scintillation efficiency, energetic resolution, n/γ -discrimination FOM, microhardness by Vickers (HV) and stability of polystyrene based PS samples with different content

№ PS	PS content (wt%)	Rel. LY (%)	Energy resolution (%)	HV (MPa)	FOM at 1.0 MeVee	Long-term stability
1	Standard: 2% paraterphenyl + 0.05% POPOP	100	5.9	231	<0.5	Years
2	40% tert-BuPPD + 0.1% POPOP	90	6.2	182	1.67	Years
3	40% m-DMePPD + 0.1% POPOP	96	6.0	150	1.22	Years
4	36% PPO + 0.1% DPA	89	6.2	24	2.41	7–10 days

PPO molecule (Table 1), that creates considerable steric hinderences for molecule diffusion in polymer. Thus the PS with 40% TBPPD and 40% DMePPD have the significantly higher microhardness (HV = 135 i 73 MPa, respectively), than PS with 36% PPO.

Opposite behavior of n/γ -discrimination and mechanical strength, as it was noticed above, is attributed to activator concentration increase, n/γ -discrimination improves due to increase of triplet-triplet annihilation probability and the microhardness reduces due to activator concentration increase leads to change of hard structure polymer matrix with soft amorphous substance (the plasticization effect). Wherein, the rate of microhardness decrease with activator content increase depends on affinity of the activator substance to polymer matrix and on structure of alkyl substitutes.

Thus, in a PS with high activator content (up to 40 wt%), possibility to increase the microhardness by use of activators with high affinity to polymer matrix rise up. At the same time, FOM decrease in PS with alkyl-substituted activators means that alkyl-substitutes create steric hindrances for close approach of chromophore groups of the molecules. Than reduces probability of triplet migration and reduces triplet-triplet annihilation probability. In such a case it leads to increase of more delayed components the pulse intensity. However, despite some FOM reduction, the polystyrene based PS material with 40% tert-BuPPD + 0.1% POPOP content is similar in mechanical and other properties to well known polystyrene based PS with standard content mark UPPS-923A [20]. This material, as 40% TBPPD, is capable to polymerization in big volume, to be easily tooled and polished, and has the high transparency and hardness and long-term stability.

Presented results of PS with n/γ -discrimination demonstrate ability of such scintillators use in practice. For monitoring and radiometry of fast neutrons the most important parameter is the frequency of false counts in the neutron channel (F_n) which is calculated as: $F_n = N_n/N_\gamma$, where N_n —the number of false counts in the neutron channel for the time T ; N_γ —the number of counts in γ -channel, registered for the same time.

The parameter F_n was measured for two PS: 40% TBPPD and 36% PPO. The samples were irradiated with electrons and γ -rays from a strontium-yttrium source Sr-90 similar to the measurements with Pu-Be source (Figs. 11 and 13). The registration threshold was 150 keVee, the counting ments ate—960 pulse/s.

The measurement results are presented at Fig. 16 as $Q_{\text{slow}}/\langle Q_{\text{slow}} \rangle$ dependence on Q_{total} for the PS 40% TBPPD (a) and 36% PPO (b). $\langle Q_{\text{slow}} \rangle$ is presented at Fig. 2a, c respectively. It is obvious, the line $\langle Q_{\text{slow}} \rangle$ on Q_{total} , which in Fig. 11 separates neutrons and γ -rays experimental dots groups, in Fig. 16 (as at Fig. 13) transforms to horizontal line with ordinate $Q_{\text{slow}}/\langle Q_{\text{slow}} \rangle = 1$. Also, it is obvious, the γ -rays group practically does not intersect with the area $Q_{\text{slow}}/\langle Q_{\text{slow}} \rangle > 1$. Thus, at the total events quantity $N_\gamma = 73,300$, registered in whole energy diapason with the PS 36% PPO, only few events ($N_n = 5$) are located in the neutron area and are false (Fig. 16a). For the PS 40% TBPPD (Fig. 16b) with the total events number $N_\gamma = 230,510$, the fail events $N_n = 120$. If to place these data into expression $F_n = N_n/N_\gamma$, it can be found, for the PS 36% PPO the fail counts frequency in the neutron channel amounts $F_n = 1/14,660$ or 0.0068%, and for the PS 40% TBPPD— $F_n = 1/1921$ or 0.052%.

These data confirm ability of PS development with n/γ -discrimination. They can be used for parameters and can be used for production of detectors for the fast neutrons registration through the γ -ray background.

4 Conclusion

The success of polymer compositions creation capable to effectively detect neutrons in the presence of a gamma background depends on the ability to convert the excitations energy. It is shown that for the implementation of this scenario, either organometallic complexes can be used, as centers for trapping the triplet excitation energy or transforming energy by triplet-triplet annihilation. Each of the ways has its merits but from

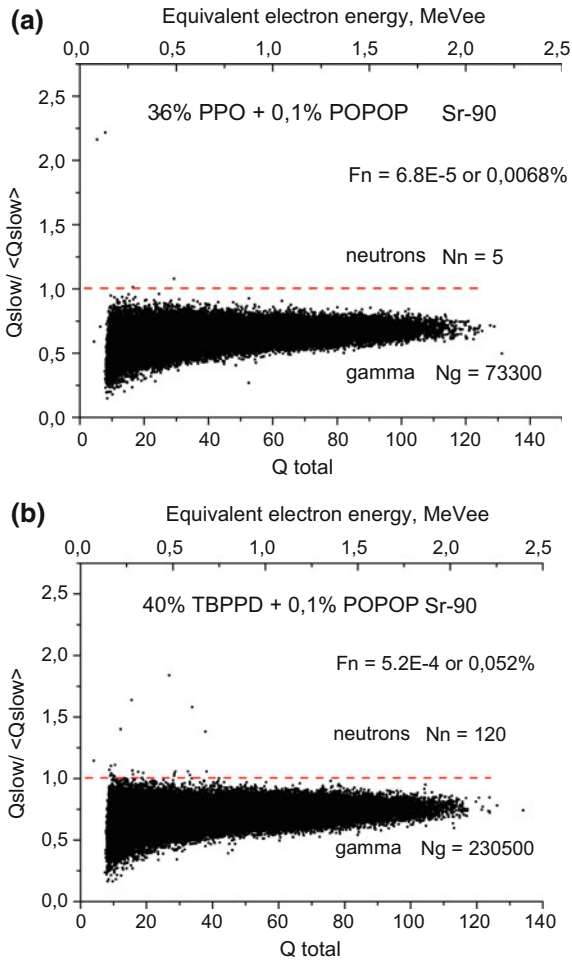


Fig. 16. Dependence of $Q_{slow}/\langle Q_{slow} \rangle$ on Q_{total} for PS: **a** 40% TBPPD; **b** 36% PPO, obtained by registration of electrons and γ -rays from a strontium–yttrium source Sr-90. $\langle Q_{slow} \rangle$ is calculated from data Fig. 2a, c. The dashed line at $Q_{slow}/\langle Q_{slow} \rangle = 1$ shows the border, separating neutrons and γ -rays areas. The registration threshold is 150 keVee. The count rate—960 count/s

the point of view of the achieved results, the transformation by the triplet-triplet annihilation is more preferable. For phenomena implementation to practice it is necessary to enrich polymer with activator to a level corresponding to mechanical strength of PS. To overcome these difficulties, it is necessary to use activators with a modified structure. Finally the plastic with good neutron—gamma separation parameter are obtained. The developed PS with the high n/γ -discrimination, good microhardness and long-term stability has to be transferred to industrial scale production that makes such scintillators an actual for new neutron detector design and engineering.

References

1. J.B. Birks, in: *The Theory and Practice of Scintillation Counting* (Pergamon Press, 1964)
2. W. Daenhick, R. Sherr, Pulse shape discrimination in stilbene scintillators. *Rev. Sci. Instrum.* **32**(6), P666 (1961)
3. A. Suhami, D. Ophir, On pulse shape discrimination in anthracene. *Nucl. Instrum. Methods* **30**, 141–144 (1964)
4. N. Zaitseva, J. Newby, S. Hamel, L. Carman, M. Faust, V. Lordi, N.J. Cherepy, W. Stoeffl, S.A. Payne, Neutron detection with single crystal organic scintillators. *Proc. SPIE* **7449**, 744911–(1–10) (2009)
5. N. Zaitseva et al., Plastic scintillators with efficient neutron/gamma pulse shape discrimination. *Nucl. Instrum. Methods Phys. Res. A* **668**, 88–93 (2012)
6. K. Peuckert, Investigation of the decay properties of organic scintillators stimulated by γ -rays, protons, or α -particles. *Nucl. Instrum. Methods* **17**, 257–260 (1962)
7. E. Bovet, P. Boschung, J. Rossel, Light response and pulse shape discrimination properties for NE 232. *Nucl. Instrum. Methods* **101**, 315–319 (1972)
8. A.F. Adadurov, P.N. Zhmurin, V.N. Lebedev, V.N. Kovalenko, Plastic scintillators with β -diketone Eu complexes for high ionizing radiation detection. *Appl. Radiat. Isot.* **69**, 1475–1478 (2011)
9. A.F. Adadurov, P.N. Zhmurin, V.N. Lebedev, V.V. Kovalenko, Plastic scintillator with phosphorescent dopants for α -particles registration. *Nucl. Instrum. Methods Phys. Res. A* **621**, 354–357 (2010)
10. P.N. Zhmurin, V.N. Lebedev, A.F. Adadurov, V.N. Pereymak, Yu.A. Gurkalenko, Plastic scintillator for pulse shape neutrons and gamma quanta discrimination. *Radiat. Meas.* **62**, 1–5 (2014)
11. P.N. Zhmurin, V.N. Lebedev, A.F. Adadurov, V.N. Pereymak, Yu.A. Gurkalenko, Pulse shape neutrons and gamma quanta discrimination by means of plastic scintillator of the new generation. *Funct. Mater.* **20**(4), 500–503 (2013)
12. P. Blanc, M. Hamel, C. Dehé-Pittance, L. Rocha, R.B. Pansu, S. Normand, Neutron/gamma pulse shape discrimination in plastic scintillators: preparation and characterization of various compositions. *Nucl. Instrum. Methods Phys. Res. A* **750**, 1–11 (2014)
13. C.L. Morris, A digital technique for neutron-gamma pulse shape discrimination. *Nucl. Instrum. Methods* **137**, 397–398 (1976)
14. J.H. Heltsley et al., Particle identification via pulse-shape discrimination with a charge-integrating ADC. *Nucl. Instrum. Methods Phys. Res. A* **263**, 441–445 (1988)
15. S. Nutter, C.R. Bower et al., Sintered Halon as a diffuse reflecting liner for light integration boxes. *Nucl. Instrum. Methods Phys. Res. A* **310**, 665–670 (1991)
16. R.A. Winyard et al., Pulse shape discrimination in inorganic and organic scintillators. *Nucl. Instrum. Methods* **95**, 141–153 (1971)
17. Stopping powers for electrons and positrons. ICRU report 37; International commission on radiation units and measurements, Bethesda, Maryland, USA, pp. viii + 267 (1984)
18. P.N. Zhmurin, V.N. Lebedev, V.D. Titskaya, A.F. Adadurov, D.A. Elyseev, V.N. Pereymak. Polystyrene-based scintillator with pulse-shape discrimination capability. *Nucl. Instrum. Methods Phys. Res. A* **761**, 92–98 (2014)
19. P.N. Zhmurin, V.N. Lebedev, V.D. Titskaya, A.F. Adadurov, D.A. Elyseev, V.N. Pereymak, Polystyrene-based plastic scintillator for n/γ -discrimination. *Funct. Mater.* **21**(3), 282–289 (2014)
20. A. Artikov et al. Properties of the Ukraine polystyrene-based plastic scintillator UPS 923A. *Nucl. Instrum. Methods Phys. Res. Sect. A* **555**, 125–131 (2005)